American Journal of Engineering Research (AJER)
e-ISSN: 2320-0847 p-ISSN : 2320-0936
Volume-11, Issue-10, pp-59-67
www.ajer.org
Research Paper Open Access

Monitoring the Effect of Land Cover Changes on Land Surface Temperature (LST) in Mojokerto, Indonesia Using Multi-temporal Landsat-8 Imagery

[1]Abdi Sukmono, [1,2]Ade Irmasari, [1]Firman Hadi,&[1]Nurhadi Bashit
[1]*Department of Geodetic Engineering, Diponegoro University, Semarang, Indonesia*
[2]*National Land Agency-Mojokerto Office, Mojokerto, Indonesia*
Email: abdi.sukmono@lecturer.undip.ac.id

***ABSTRACT**: Mojokerto Regency in 2020 experienced an increase in population from the previous year by 0.15% because this regency was in the period of development of large industrial areas and new urban areas. The land cover of vegetation and water has decreased drastically every year. It is inversely proportional to the land cover of built-up areas and bare land which has increased, thereby triggering an increase in land surface temperature. It is an important parameter in the physical processes and interactions between the soil and the atmosphere. In this study, the extraction of land surface temperature was carried out through image processing on the Landsat-8 thermal band which has a spectral filter of two TIRS channels with a narrower bandwidth to capture better ground surface information. The method employed in this study was temperature extraction using Split-Window (SW) and Mono-Window (MW) algorithms. The SW algorithm can eliminate atmospheric effects through differential atmospheric absorption, while the MW algorithm only requires two atmospheric parameters, namely transmittance and average atmospheric temperature. The estimated accuracy of land surface temperature on Landsat-8 imagery in Mojokerto Regency was indicated by the RMSE values of 2.971°C for the Split-Window algorithm, 5.5°C for the band-10 Mono-Window algorithm, and 5.616°C for the band-11 Mono-Window algorithm. Land cover data processing was carried out using a supervised classification with the maximum likelihood method which divided the land cover into vegetation, waters, built-up land, and bare land. We also used a grid size of 30" × 30" for the calculation of land cover area and average temperature. Regression was carried out to find out whether the variable of land cover affected the increase in the land surface temperature of the soil in Mojokerto Regency. In 2017, the coefficient of determination was 0.626 from the regression between the land surface temperature of the soil and land cover. In 2019, it became 0.602. Furthermore, in 2021, the coefficient of determination was still 0.602. It means that, in these periods, the influence of land cover on the land surface temperature of the soil has a high degree of relationship.*
***KEYWORDS**: Land Surface Temperature, Landsat-8, Split-Window, Mono-Window, Land Cover.*

Date of Submission: 07-10-2022 Date of acceptance: 23-10-2022

I. INTRODUCTION

Global warming has received enough attention to become a hot topic discussed among the public. This is because global warming has a tremendous impact on the earth, in which the land surface temperature on earth increases every year. Based on data obtained from the World Meteorological Organization (WMO), the global average of land surface temperature in 2020 increased by 1.2 ± 0.1 degrees Celsius from the pre-industrial period in 1850-1900, making the current decade the hottest on record from previous years.

Global warming causes climate change, which can affect the increase in land surface temperature. The study of land surface temperature can be used to determine the magnitude of the temperature value in several places. Land surface temperature is an important parameter in physical processes and interactions between soil and atmosphere [1]. The negative impact of the development of urban areas and industrialization is the decline in environmental quality which triggers an increase in air temperature [2]. An increase in temperature can also be triggered by changes in landform, such as a decrease in the amount of vegetation density, an increasing rate of population growth, and uncontrolled urban development. Changing the form of vegetation land into built-up land will have an impact on variations in atmospheric dynamics and climate change.

The extraction of land surface temperature can be obtained from image processing on the Landsat-8 thermal band because it has the advantage of displaying images with a sensitivity of 16 bits, thereby making objects easier to be distinguished. In addition, Landsat-8 imagery also supports prolonged research because it is freely available and contains multi-temporal data [3]. The spectral filter of the two TIRS channels provides a narrower bandwidth which can capture ground-level information better.

Many algorithms have been proposed and developed to estimate the land surface temperature of the soil. The Landsat-8 TIRS sensor has two spectrally adjacent thermal channels. It is considered appropriate for the Split-Window (SW) algorithm. The basis of the SW algorithm is that the emission attenuation for atmospheric absorption is proportional to the emission difference from simultaneous measurements at two different wavelengths. Each can be used for a different amount of atmospheric absorption [4]. The SW algorithm can eliminate atmospheric effects through differential atmospheric absorption and obtain LST values from a linear or nonlinear combination of the brightness temperatures of two adjacent channels centered at 11 and 12 micrometers. Considering that this algorithm does not require accurate information about the atmospheric profile during satellite acquisition, it has been widely used in LST retrieval from several sensors due to its simplicity and robustness [5]. If compared to several atmospheric parameters required in the second correction method, the Mono-Window (MW) algorithm only requires two atmospheric parameters (i.e., transmittance and average atmospheric temperature) for LST retrieval.

Mojokerto Regency is one of the most developed regencies with a population of 1,119,209 people. According to data from Indonesia's Central Statistics Agency, Mojokerto Regency in 2020 experienced an increase in the percentage of the population of around 0.15% from the previous year. Based on the Medium-Term Infrastructure Investment Development Plan (Indonesian: *Rencana Pembangunan Investasi Infrastruktur Jangka Menengah* (RPI2JM)) of Mojokerto Regency concerning the Residential Area Development Plan (Indonesian: *Rencana Pembangunan dan Pengembangan Kawasan Permukiman* (RP2KP)) of Mojokerto Regency in 2015-2034, this regency has strategic issues in the development of settlements and urban infrastructure to support potential economic activities.

The method used in this research was the extraction process of land surface temperature based on the calculation of the Split-Window (SW) and Mono-Window (MW) algorithms. It was followed by field validation to get the best algorithm and statistical tests to obtain the error value of each algorithm. The results of the estimation of land surface temperature with the algorithm that had better accuracy were regressed with a land cover map and processed through supervised classification to find out whether land cover influenced land surface temperature in Mojokerto Regency.

II. MATERIALS AND METHODS

2.1. Research Location

This study was conducted in Mojokerto Regency, East Java Province, Indonesia. It is a developing region in Indonesia, especially in its industrial sector. As a result, there is a significant change in land cover from year to year in this region. Topographically, Mojokerto Regency is divided into three morphological units, namely mountains in the south, structural hills in the north, and plains covering the central and northern regions. The topography of Mojokerto Regency tends to be concave in the middle and high in the south and north. The southern part is a fertile mountainous area, covering the Districts of Pacet, Trawas, Gondang, and Jatirejo. The middle part is a land area, while the northern part is a limestone hill which tends to be less fertile. Based on the relief and the shape of the slopes, this area is divided into three classes of slopes, namely a low level with a slope of 0-2% covering an area of 409,885 km^2 which is dominated by valley areas located in the north and center, a medium level with slopes of 2-15% covering an area of 454,795 km^2 located in the north and extending to several locations in the south, and a high level with a slope between 15% and ≥ 40% covering an area of 2,290,657 km^2 in the south which is dominated by mountains.

Mojokerto Regency is located at an altitude between 0 and 3,156 MASL (meters above sea level). Topographically, it consists of lowlands, highlands, and hills. In lowland areas, it has an altitude of 0-23 MASL. Hilly areas have an altitude of 23-150 MASL. At last, the highlands have an altitude of 150-3,156 MASL.

Fig 1. Research Location in Mojokerto, Indonesia

The research location was in Mojokerto Regency, specifically in three districts: Ngoro, Pacet, and Trawas. The determination of the research location was based on the land cover in the three districts which was quite complete and varied, which could represent other districts throughout Mojokerto Regency. The land cover consists of built-up land, open land, vegetation, and water bodies.

2.2. Materials

The materials used in this study were as follows.

a) Landsat-8 imagery for 9 September 2017, 10 October 2019, and 22 October 2021
b) In-situ land surface temperature data taken on October 8-29, 2021, from 09.00 to 11.00
c) Field validation data of land cover
d) Topographic map of Mojokerto Regency with a scale of 1:25,000
e) Data of Mojokerto Regency administrative boundary

2.3. The Estimation Algorithms for Determining Land Surface Temperature with Landsat-8 Imagery

Land surface temperature (LST) is a temperature state affected by surface energy, the nature of the surface, and the atmosphere in the region. The purpose of determining land surface temperature is to find out the average temperature condition of the ground surface which is defined in the scope of one pixel. The detection of land surface temperature was carried out using the basic principles of the physics of light. Meanwhile, in Landsat-8 imagery, LST analysis can be conducted using the TIRS channel, which is the most sensitive channel to changes in temperature using the brightness temperature conversion formula as listed in equation II.6 [6]. The land surface temperature of the soil can be obtained by processing Landsat-8 satellite image data based on the spectral radiance value of the thermal infrared channel in band 10. SW has the lowest sensitivity to input parameter errors. Moreover, errors in parameters will have less impact on results in a humid environment. According to Wang [7], concerning the results of the sensitivity analysis, SW is the most stable method, in which errors in the input parameters do not cause large errors in LST. Meanwhile, MW has the highest sensitivity in humid environments and high temperatures. Furthermore, MW is very sensitive to errors in the content of water vapor in the atmosphere. However, the more input parameters are, the lower the probability of LST error will be. The MW method is more sensitive to errors in input parameters, especially in hot and humid conditions, and more sensitive to errors in the moisture content of the atmosphere. MW is also sensitive to average effective atmospheric temperature errors.

Furthermore, the algorithms for determining land surface temperature with Landsat-8 imagery used in this study were the Mono-Window and Split-Window algorithms, as described further in the following.

A. Split-Window (SW) Algorithm

The data used to estimate the land surface temperature is the brightness temperature value obtained from the ToA value on the 10-radian channel of the Landsat-8 imagery from the TIRS sensor and the surface emissivity value obtained from the vegetation proportion value determined from the NDVI value [8]. The steps for calculating this algorithm are as follows.

a) *Calculating Brightness Temperature (BT)*

$$BT = \frac{K_2}{ln\left(\frac{K_1}{L_\lambda}+1\right)} - 273{,}15 \quad \text{..... (1)}$$

Where:
BT = ToA of atmosphere brightness temperature (°Celsius)
L = ToA of spectral radiance (Watt/m^2srad µm)
K_1 = band-specific thermal conversion constant from the metadata
K_2 = band-specific thermal conversion constant from the metadata

b) Calculating NDVI

$$NDVI = \frac{Band\ 5 - Band\ 4}{Band\ 5 + Band\ 4} \quad \text{..... (2)}$$

Where:
Band 4 = red channel on Landsat-8
Band 5 = near-infrared channel on Landsat-8

c) *Calculating the Proportion of Vegetation (PV)*

$$PV = \left(\frac{NDVI - NDVIsoil}{NDVIveg - NDVIsoil}\right)^2 \quad \text{..... (3)}$$

Where:
NDVI =previously obtained NDVI value
$NDVI_{soil}$ =NDVI value for soil
$NDVI_{veg}$ =NDVI value for vegetation

d) *Calculating Land Surface Emissivity (LSE)*

$$LSE = \varepsilon v * PV + \varepsilon s * (1 - PV) \quad \text{..... (4)}$$

Where:
PV = Nilai PV yang sebelumnya telah diperoleh
εs =soil emissivity in bands 10 and 11
εv =vegetation emissivity in bands 10 and 11

e) *Calculating Land Surface Temperature (LST)*

$LST = BT10 + C1(BT10 - BT11) + C2 (BT10 - BT11)^2 + C0 + (C3 + C4W) * (1 - LSE) + (C5 + C6W) * \Delta LSE$ ..... (5)

Where:
LST : land surface temperature (°C)
$C_0 - C_6$: Split Window coefficient
$BT_{10\text{-}11}$: brightness temperature (°C) in bands 10 and 11
LSE : the average LSE value of bands 10 and 11
W : atmospheric water vapor content = 0.013 (Latif, 2014)
ΔLSE : the difference between the value of LSE band 10 and the value of LSE band 11

B. Mono-Window (MW) Algorithm

This algorithm requires the value of land surface emissivity, atmospheric transmission, and the average effective temperature of the atmosphere. The steps for calculating this algorithm are as follows.

1. Determining the Band Coefficient

$$Ci = \varepsilon i . \tau i \quad \text{..... (6)}$$

Where:
Ci = coefficient of the band *i*
εi = the surface emissivity of the band *i*
τi = atmospheric transmission of the band *i*

2. *Calculating the Coefficient of Determination*

$$Di = (1 - \tau i . [1 + (1 - \varepsilon i) . \tau i \quad \text{..... (7)}$$

Where:
Di = determination of band *i*
εi = the surface emissivity of the band *i*
τi = atmospheric transmission of the band *i*

3. *Calculating Land Surface Temperature (LST)*

$$Ts = \frac{ai(1-Ci-Di)+[bi(1-Ci-Di)+Ci+Di]Ti-DiTa}{Ci} \quad \text{..... (8)}$$

T_s = the land surface temperature of the soil
T_i = brightness temperature (BT)
T_a = the average effective temperature of the atmosphere (°C)

2.4. Algorithm for Classifying Land Cover

Land cover is a physical material on the earth's surface [9]. It is the material we can see. In addition, the material directly interacts with electromagnetic radiation and causes the reflected energy level that we observe as a digital tone or number for a location on a satellite image. Land cover includes grass, roads, trees,

bare soil, water, and others. Land cover classification in satellite imagery in this study was carried out by machine learning with supervised classification. Supervised classification is a classification carried out under the direction of an analyst (supervised), in which the criteria for grouping classes are determined based on class signatures obtained through the creation of a training area [10, 11].

According to Marini [12], supervised classification is a method needed to transform multispectral image data into classes of spatial elements in the form of thematic information. The supervised classification method begins with the creation of a sample area to determine class characteristics. This activity is to identify prototypes (clusters) of several pixels that represent each desired class or category by determining the position of the sample in the field with the help of a land cover map as a reference for each class.

III. RESULTS AND DISCUSSION

3.1. Monitoring Land Surface Temperature Changes

Based on the distribution of land surface temperature generated from Landsat-8 image processing in 2017, 2019, and 2021, seven LST classes can be made using the statistical formula put forward by Triyanti (2008 in Suri, 2018) in her research on land surface temperature. The results of land surface temperature for multi-temporal development can be seen in Figures 2, 3, and 4.

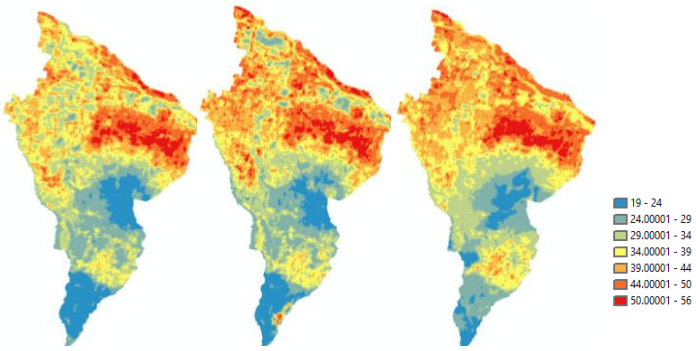

(a)In 2017 (b)In 2019 (c)In 2021

Fig 2. Multi-temporal Development of Land Surface Temperature (°C) in the SW Algorithm

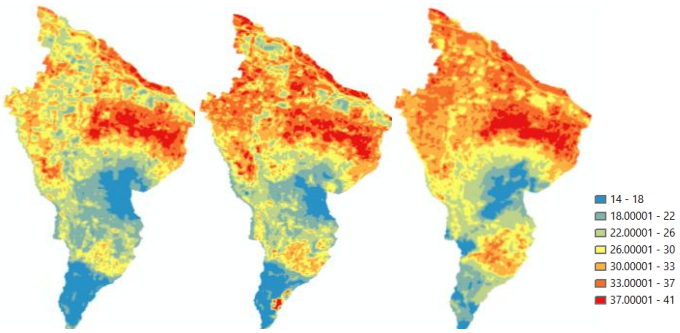

(a)In 2017 (b)In 2019 (c)In 2021

Fig 3. Multi-temporal Development of Land Surface Temperature (°C) in the Band-10 MW Algorithm

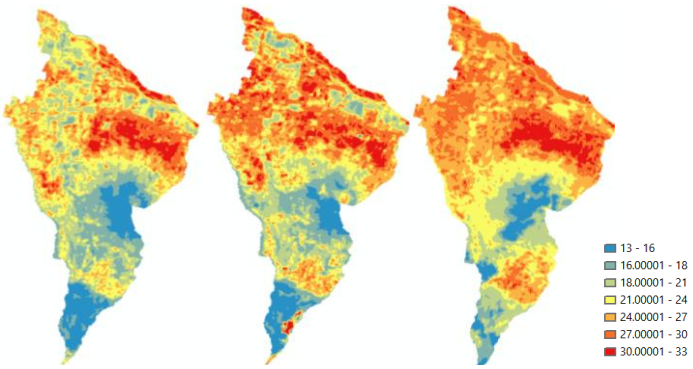

(a)In 2017 (b)In 2019 (c)In 2021

Fig 4. Multi-temporal Development of Land Surface Temperature (°C) in the Band-11 MW Algorithm

This study revealed that in areas with more vegetation cover in hilly and mountainous areas to the south, the temperature is low. High temperatures are marked by red color in the area of built-up land which is increasingly expanding, that was initially only centered in the industrial area, but then expanded to the west.

Data validation was carried out to obtain the best algorithm with the highest accuracy value or the lowest root mean square error (RMSE). The RMSE value for the SW algorithm is 2.971°C, the RMSE value for the band-10 MW algorithm is 5.5°C, and the RMSE value for the band-11 MW algorithm is 5.616°C. Therefore, the best algorithm for extracting the land surface temperature of the soil in this study is the SW algorithm. The results of land surface temperature processing using the SW algorithm were used for further analysis. The description of the results of the SW algorithm validation can be seen in Table 1 below.

Table1. The Calculation of RMSE using the SW Algorithm

In-situ (°C)	SW (°C)	Difference (°C)	Difference^2 (°C)
32.167	34.868	-2.701	7.298
31.200	33.909	-2.709	7.336
30.700	34.192	-3.492	12.193
30.800	35.904	-5.104	26.053
30.100	33.899	-3.799	14.433
30.333	33.996	-3.663	13.418
30.100	33.919	-3.819	14.584
30.133	37.104	-6.970	48.584
30.467	35.736	-5.269	27.766
31.300	34.477	-3.177	10.093
⋮	⋮	⋮	⋮
53.467	49.260	4.206	17.694
Total			**1,076.994**
RMSE			**2.971**

3.2. Monitoring Land Cover Changes

The land cover processing using the supervised classification method of nearest neighbor analysis resulted in four macro classes of land cover, consisting of vegetation, water bodies, built-up land, and bare land, as shown in Figure 5.

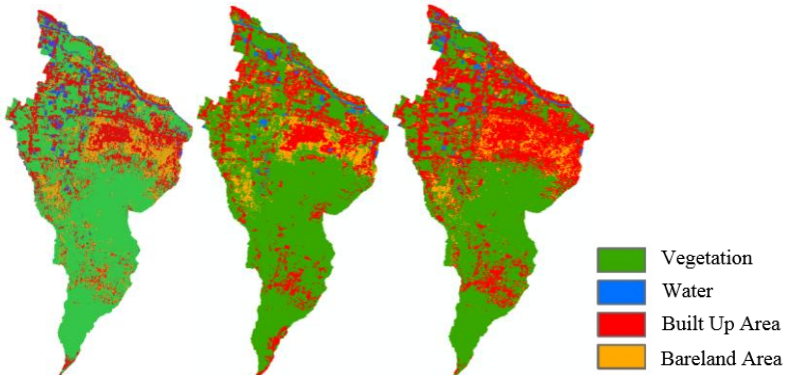

(a)In 2017 (b)In 2019 (c)In 2021

Fig 5. Development of Multi-temporal Land Cover Based on Supervised Classification

Table 2. Multi-temporal Land Cover Area Based on Supervised Classification

Land Cover	Total Area (Ha)		
	2017	2019	2021
Vegetation	10,604.25	11,819.43	9,695.61
Water	743.31	417.87	438.66
Built Up Area	4,201.74	4,127.94	6,504.48
Bare Land Area	2,242.35	1,426.41	1,152.9

The results of the land cover validation were made in the 2021 confusion matrix table which obtained an overall accuracy value of 81.58% with a kappa coefficient of 0.786. As seen in Figure 7, Mojokerto Regency is dominated by land cover with the types of vegetation and built-up land. Based on Table 2, the land cover of vegetation and water has decreased every year. It is inversely proportional to the land cover of built-up areas and

bare land which has increased. This is due to the increasing development for industrial purposes or in the context of developing regional development to become new urban areas.Based on the Medium-Term Infrastructure Investment Development Plan (Indonesian: *Rencana Pembangunan Investasi Infrastruktur Jangka Menengah* (RPI2JM)) of Mojokerto Regency concerning the Residential Area Development Plan (Indonesian: *Rencana Pembangunan dan Pengembangan Kawasan Permukiman* (RP2KP)) of Mojokerto Regency in 2015-2034, this regency has strategic issues in the development of settlements and urban infrastructure to support potential economic activities, especially in Ngoro and Trawas Districts.

3.3. Analyzing the Effect of Land Cover Changes on Land Surface Temperature

For analyzing the influence of land cover on land surface temperature, the researchers used the unit area analysis method with a grid of variance scales followed by the regression method to determine the effect. The grid in this study aimed to provide the boundaries in the research area so that, when analyzing between regions, the information contained in the research area can be conveyed properly. The choice of grid size was based on the size of the research area, in which the total area of the three districts that become the research locations is around 135.48 km^2. For this reason, the grid created was presented with a resolution of 30" × 30" or 900 meters × 900 meters with a total of 271 grid plots adjusted to the research location. Furthermore, the distribution of the grids in the research area can be seen in Figure 6.

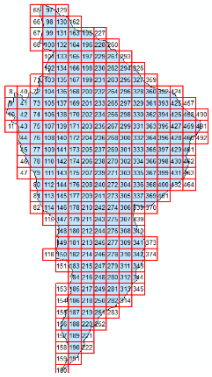

Fig 6. Grids with a Size 30" × 30"

The total land cover area in one grid when fully occupied is 81 hectares. An unfilled or empty value means that the grid does not contain a certain type of land cover. For example, in table 3, in grid number 9, there is no value or empty land cover type. It means that, in grid number 9, there is no type of land cover in the water body so that the value is 0 (zero).

Table 3. Land Cover Area in 2021

Grid Number	Land Cover Area in 2021 (Ha)			
	Water	Bare Land	Built-Up Area	Vegetation
8			1.519	6.778
9		0.752	19.438	29.516
10	1.246	0.248	30.636	13.221
11	2.488		1.915	4.964
40		0.109	3.474	9.280
42		1.794	18.503	60.703
43		0.756	17.001	59.489
44	1.619	0.941	20.895	47.638
45	0.996	0.270	25.561	25.550
⋮	⋮	⋮	⋮	⋮
271			0.521	1.670

The results of the calculation of the average value of the land surface temperature of the soil on each grid will be used as an independent variable in the regression analysis.

Table 4. Land Cover Area in 2021

Grid Number	Temperature (°C)	
	Mean	St. dev
8	38.733	1.427
9	39.684	2.632
10	40.859	1.835
11	38.933	1.587
40	39.857	1.542
41	40.846	1.891
42	40.605	1.289
43	40.040	1.254
44	38.375	1.293
45	36.940	1.526
⋮	⋮	⋮
21	37.467	1.670

This study used multiple linear regression to obtain information about to what extent the independent variable (i.e., land cover) affects the dependent variable (i.e., the land surface temperature of the soil) with a significance level of 0.05. The dependent variable in this study consisted of three types of land cover: vegetation (X1), built-up land (X2), and bare land (X3), while the independent variable was the land surface temperature (Y).

Table 5. The Regression of Land Cover and Land Surface Temperature of the Soil

Year	Equation	R^2	Correlation
2017	$Y = 37.320 - 0.066\ X_1 + 0.108\ X_2 + 0.021\ X_3$	0.626	0.791
2019	$Y = 37.836 - 0.072\ X_1 + 0.099\ X_2 + 0.016\ X_3$	0.602	0.776
2021	$Y = 40.286 - 0.086\ X_1 + 0.038\ X_2 + 0.067\ X_3$	0.602	0.776

The multi-temporal regression performed had a significant value less than an alpha value of 0.05. Based on Table 5, especially concerning the correlation values obtained, it can be concluded that the land cover of the independent variables "vegetation (X1)", "built-up land (X2)", and "open land (X3)" has an effect and a strong level of relationship on changes in temperature in Mojokerto Regency in 2017, 2019, and 2021.

IV. CONCLUSION

Based on the analysis of the research results that have been carried out, it can be concluded as follows.

A. The estimated accuracy of land surface temperature on Landsat-8 imagery in Mojokerto Regency was indicated by the RMSE values of 2.971°C for the Split-Window algorithm, 5.5°C for the band-10 Mono-Window algorithm, and 5.616°C for the band-11 Mono-Window algorithm. Statistical testing proves that the three processing algorithms are significant because the obtained *p*-values are less than 0.05. Therefore, it is concluded that three processing methods using the algorithm can be used to extract the land surface temperature of the soil. However, the best algorithm in this study was the Split-Window algorithm.

B. Land cover affects the land surface temperature of the soil in Mojokerto Regency. In 2017, the coefficient of determination was 0.626. In 2019, it became 0.602. Furthermore, in 2021, the coefficient of determination was still 0.602. It means that, in these periods, the influence of land cover on the land surface temperature of the soil has a high degree of relationship.

REFERENCES

[1]. Faridah, S. A. N., & Krisbiantoro, A. (2014). Analisis Distribusi Temperatur Permukaan Tanah Wilayah Potensi Panas Bumi Menggunakan Teknik Penginderaan Jauh Di Gunung Lamongan, Tiris-Probolinggo, Jawa Timur. Berkala Fisika, 17(2), 67–72.

[2]. Dede, M. (2019). Dinamika Suhu Permukaan Dan Kerapatan Vegetasi Di Kota Cirebon. Jurnal Meteorologi Klimatologi dan Geofisika, 6(1), 23–31. https://doi.org/10.36754/jmkg.v6i1.111

[3]. Adi, M. N., & Sudaryatno. (2014). Pemanfaatan Citra Landsat 8 Untuk Penentuan Zonasi Kekeringan Pertanian Di Sebagian Kabupaten Grobogan Dengan Metode TVDI (Temperature Vegetation Dryness Index). Jurnal Bumi Indonesia, 3(4), 1–10.Forero, N., Hernández, J., Gordillo, G.: Development of a monitoring system for a PV solar plant. Energy Conversion and Management 47(15-16), 2329–2336 (2006).

[4]. Yu, X. (2014). Land surface temperature retrieval from landsat 8 TIRS-comparison between radiative transfer equation-based method, split window algorithm and single channel method. Remote Sensing, 6(10), 9829–9852. https://doi.org/10.3390/rs6109829
[5]. Du, C.. (2015). A practical split-window algorithm for estimating land surface temperature from landsat 8 data. Remote Sensing, 7(1), 647–665. https://doi.org/10.3390/rs70100647
[6]. USGS. (2019). Landsat 8 (L8) Data Users Handbook Version 5.0. South Dakota: Department of Interior USGS.
[7]. Wang, L.. (2019). Comparison of three algorithms for the retrieval of land surface temperature from landsat 8 images. Sensors (Switzerland), 19(22). https://doi.org/10.3390/s19225049
[8]. Latif, M. S. (2014). Land Surface Temperature Retrival of Landsat-8 Data Using Split Window Algorithm- A Case Study of Ranchi District. Internal Journal of Engineering Development and Research, 2(4), 3840–3849.
[9]. Fisher, Peter. (2005). Land Use and Land Cover: Contradiction or Complement. Re-Presenting GIS, January, 85–98.
[10]. Sampurno, R. M., & Thoriq, A. (2016). Klasifikasi Tutupan Lahan Menggunakan Citra Landsat 8 Operational Land Imager (OLI) Di Kabupaten Sumedang. Jurnal Teknotan, 10(2–3), 61–70. https://doi.org/10.1016/s0376-7388(00)85017-6
[11]. Kiefer, & Lillesand. (1979). Penginderaan Jauh dan Interpretasi Citra. Yogyakarta: Gajah Mada University Press.
[12]. Marini, Y.(2014). Perbandingan Metode Klasifikasi Supervised Maximum Likelihood Dengan Klasifikasi Berbasis Objek Untuk. Prosiding Seminar Nasional Penginderaan Jauh 2014, November, 505–516.